

**$\alpha$  cluster condensation in  $^{12}\text{C}$  and  $^{16}\text{O}$ ?**Y. Suzuki<sup>1</sup> and M. Takahashi<sup>2</sup><sup>1</sup>*Department of Physics, Niigata University, Niigata 950-2181, Japan*<sup>2</sup>*Graduate School of Science and Technology, Niigata University, Niigata 950-2181, Japan*

(Received 22 January 2002; published 10 June 2002)

The possibility of  $\alpha$  cluster condensation has recently been suggested for some states of  $^{12}\text{C}$  and  $^{16}\text{O}$  lying near the  $3\alpha$  and  $4\alpha$  thresholds, respectively. An  $\alpha$ -boson model was applied to examine this issue for the system of  $3\alpha$  and  $4\alpha$  particles. With the stochastic variational method, bound state solutions were obtained for both the ground and excited states. The extent of  $\alpha$  condensation was quantified by diagonalizing density matrices. The probabilities that the  $\alpha$  particles occupy an  $S$  orbit were 30–40 % for some candidate states of  $\alpha$  condensation.

DOI: 10.1103/PhysRevC.65.064318

PACS number(s): 21.60.Gx, 03.75.Fi, 21.45.+v, 27.20.+n

**I. INTRODUCTION**

It is well known that a cluster model is successful in describing structure of light nuclei [1,2]. The cluster model assumes that a group of nucleons forms a localized substructure. In particular, an  $\alpha$  cluster is considered to play a predominant role in the cluster model. This is because the  $\alpha$  particle is stable as is understood by its large binding energy per nucleon.

The  $\alpha$  particle behaves as a boson. An interesting question is if the Bose-Einstein condensation occurs in a system of  $\alpha$  particles. The condensation of neutral atoms such as  $^{87}\text{Rb}$  and  $^{23}\text{Na}$  is realized at very low temperature when the de Broglie wavelength of the atom is comparable with the average distance between the neighboring atoms. In the case of the finite system of  $\alpha$  particles, a realization of  $\alpha$  condensation is questionable in its ground state (g.s.) because it is dominated by a nuclear shell model. Another important difference is that the  $\alpha$ - $\alpha$  interaction is short ranged whereas the atom-atom interaction is characterized by the long-ranged van der Waals force.

An intriguing interpretation has recently been proposed for some of the states in  $^{12}\text{C}$  and  $^{16}\text{O}$  [3]. The well-known  $0^+$  states lying near  $3\alpha$  and  $4\alpha$  thresholds in these nuclei have been reinvestigated from the viewpoint of an  $\alpha$  condensation. A possible condensation has been conjectured by studying the energy surfaces obtained by a special class of variational wave functions for  $N\alpha$  clusters,

$$\mathcal{A}\{e^{-\nu(X_1^2+\dots+X_N^2)}\phi(\alpha_1)\dots\phi(\alpha_N)\}. \quad (1)$$

Here  $\phi(\alpha)$  is the internal wave function of the  $\alpha$  cluster,  $X_i$  is the center-of-mass coordinate of the  $i$ th  $\alpha$  cluster, and the Fermi statistics of the constituent nucleons is observed by the antisymmetrizer  $\mathcal{A}$ . As Eq. (1) shows, the center of each  $\alpha$  cluster follows an  $S$ -wave motion whose spatial extension is specified by a Gaussian falloff parameter  $\nu$ . A “saddle point” configuration corresponding to a large spatial extension (small  $\nu$ ) has been assigned as an indication for the condensed state. The states at the excitation energies of 7.65 (in  $^{12}\text{C}$ ) and 14.0 MeV (in  $^{16}\text{O}$ ) are, respectively, considered to be the  $\alpha$  condensed states.

These states are excited states but not the g.s. An  $\alpha$  condensation, if possible, might be realized at high excitation energy near the threshold decaying into constituent  $\alpha$  particles. It is not obvious, however, that they are condensed to a single  $S$ -wave  $\alpha$  cluster orbit. The model wave function (1) used in Ref. [3] is restricted to a special form, so it is not clear if that configuration is supported by more general and extended calculations. Instead we will show that the use of a density matrix is useful in order to quantify the degree of the  $\alpha$  condensation. The purpose of this study is to examine these questions in a precise framework in the sense of variational calculations.

It is not in the realm of a present day possibility to obtain both the ground and excited states in an *ab initio* calculation. For example, the calculation for  $^{12}\text{C}$  using the realistic charge-dependent (CD) Bonn and the Argonne V8' potentials does not reproduce the correct excitation energy of the excited  $0^+$  state [4]. In this respect, it seems reasonable to perform a phenomenological analysis by assuming the  $\alpha$  particle model.

In the next section, we define our model and present a formalism to solve a bound-state problem for few-particle systems. The basic method we use is the stochastic variational method (SVM) with correlated Gaussians [5,6]. The calculation will be done for  $3$ – $5\alpha$  systems. The  $5\alpha$  system is performed mainly for demonstrating the accuracy of the present calculation. In Sec. III, results of calculation are presented with some emphasis on an analysis of the orbits occupied by the  $\alpha$  particles. This analysis will be done by investigating the eigenvalue problem of density matrices constructed from the wave functions of the system. The calculation of the density matrix is detailed in the Appendix. Section IV draws a brief summary.

**II. MODEL**

The  $\alpha$  particle is treated as a structureless boson. We are interested in states with total orbital angular momentum  $L=0$  and parity  $\pi=+$ . The quality of a variational solution crucially depends on a trial function. A variational solution  $\Psi$  for  $N\alpha$  system is obtained in terms of a combination of correlated Gaussians  $G$ ,

$$\Psi = \sum_{i=1}^{\mathcal{K}} C_i \mathcal{S}G(A_i, \mathbf{x}), \quad (2)$$

where  $\mathbf{x} = \{\mathbf{x}_1, \mathbf{x}_2, \dots, \mathbf{x}_{N-1}\}$  is a set of relative coordinates of the system. The choice of the set can be arbitrary. The set used most widely is the Jacobi coordinate system. The relative coordinates  $\mathbf{x}$  and the center-of-mass coordinate  $\mathbf{x}_N$  are related to the single  $\alpha$  particle coordinates  $\{\mathbf{r}_1, \mathbf{r}_2, \dots, \mathbf{r}_N\}$  by an appropriate transformation matrix  $U$ :

$$\mathbf{x}_i = \sum_{j=1}^N U_{ij} \mathbf{r}_j \quad (i=1, 2, \dots, N). \quad (3)$$

The symbol  $\mathcal{S}$  is a symmetrizer,  $\mathcal{S} = (1/\sqrt{N!}) \sum_{\mathcal{P}} \mathcal{P}$ , where the sum runs over all permutations  $\mathcal{P}$  of  $N$  particles.

The correlated Gaussian  $G$ ,

$$\begin{aligned} G(A, \mathbf{x}) &\equiv \exp\left(-\frac{1}{2} \sum_{ij} A_{ij} \mathbf{x}_i \cdot \mathbf{x}_j\right) \\ &= \exp\left[-\sum_{i<j} \alpha_{ij} (\mathbf{r}_i - \mathbf{r}_j)^2\right], \end{aligned} \quad (4)$$

is characterized by a symmetric, positive-definite  $(N-1) \times (N-1)$  matrix  $A$ . The matrix  $A$  is characterized by  $\frac{1}{2}N(N-1)$  elements. The diagonal elements of the matrix correspond to the nonlinear parameters of an Gaussian expansion, and the off-diagonal elements connect the different relative coordinates representing correlations between the particles. The equivalence of the two expressions in Eq. (4) for the correlated Gaussian is shown in Ref. [6]. The matrix elements  $A_{ij}$  can be expressed uniquely in terms of the elements  $\{\alpha_{kl}\}$  and vice versa.

The symmetrization of the basis function can easily be incorporated as follows. The permutation

$$\mathcal{P} = \begin{pmatrix} 1 & 2 & \cdots & N \\ p_1 & p_2 & \cdots & p_N \end{pmatrix}$$

induces a rearrangement of the single-particle coordinates as

$$\mathcal{P} \begin{pmatrix} \mathbf{r}_1 \\ \mathbf{r}_2 \\ \vdots \\ \mathbf{r}_N \end{pmatrix} = T_{\mathcal{P}} \begin{pmatrix} \mathbf{r}_1 \\ \mathbf{r}_2 \\ \vdots \\ \mathbf{r}_N \end{pmatrix}, \quad (5)$$

where the  $N \times N$  matrix  $T_{\mathcal{P}}$  is given by

$$(T_{\mathcal{P}})_{ij} = \delta_{jp_i} \quad (i, j = 1, 2, \dots, N). \quad (6)$$

With the use of Eqs. (3) and (5), we can show that the permutation  $\mathcal{P}$  acts on the correlated Gaussian as

$$\mathcal{P}G(A, \mathbf{x}) = G(\tilde{P}AP, \mathbf{x}), \quad (7)$$

where  $P$  is an  $(N-1) \times (N-1)$  matrix obtained by omitting the last row and the last column (corresponding to the

permutation-invariant center-of-mass coordinate) of the  $N \times N$  matrix  $UT_{\mathcal{P}}U^{-1}$  and  $\tilde{P}$  is its transposed matrix. Therefore the symmetrization requirement on the trial function amounts to a simple multiplication of the matrix,  $\tilde{P}AP$ . Most noticeable is that the symmetrization keeps the functional form of the correlated Gaussians.

The trial wave function of Eq. (2) contains  $\frac{1}{2}N(N-1)\mathcal{K}$  nonlinear parameters  $\{A_i\}$  as well as  $\mathcal{K}$  linear parameters  $\{C_i\}$ . An upper bound for the energy of the system is given by the eigenvalue of the generalized eigenvalue problem,

$$\sum_{j=1}^{\mathcal{K}} H_{ij} C_j = E \sum_{j=1}^{\mathcal{K}} B_{ij} C_j, \quad (i=1, 2, \dots, \mathcal{K}), \quad (8)$$

with the Hamiltonian and overlap matrices

$$\begin{aligned} H_{ij} &= \langle \mathcal{S}G(A_i, \mathbf{x}) | H | \mathcal{S}G(A_j, \mathbf{x}) \rangle, \\ B_{ij} &= \langle \mathcal{S}G(A_i, \mathbf{x}) | \mathcal{S}G(A_j, \mathbf{x}) \rangle. \end{aligned} \quad (9)$$

This equation determines the linear parameters, once the basis functions are set up.

The adequate choice of the nonlinear parameters (the elements of the matrix  $A_i$  or  $\alpha_{ij}$ ) is crucial. Although several ways for the choice of the elements of  $A_i$  have been suggested, there is no safe recipe available. While the numerical optimization would be in principle the method of choice, in practice there are several difficulties to face. The most serious ones among these are probably the large number of parameters to be optimized and the nonorthogonality of the basis states. It is very time consuming to optimize all of these parameters at once because it requires repeated calculations of both all the matrix elements,  $H_{ij}$  and  $B_{ij}$ , and the eigenvalues of Eq. (8). Due to the nonorthogonality, none of the parameter sets is indispensable, and several different choices can represent the wave functions equally well. This property makes the optimization tedious but offers the possibility of random selection of the nonlinear parameters. The SVM increases the basis dimension step by step by testing a number of candidates which are chosen randomly. Many examples have shown that this procedure is powerful to set up such a basis set that gives a virtually exact solution [5,6].

An effective potential between the  $\alpha$  particles was studied phenomenologically or by a resonating group method (RGM) [7]. We use the phenomenological potential, the  $S$ -wave potential of Ali-Bodmer [8],

$$\begin{aligned} V(r) &= 500 \exp[-(0.7r)^2] \\ &\quad - 130 \exp[-(0.475r)^2] \quad (\text{MeV}). \end{aligned} \quad (10)$$

The original Ali-Bodmer potential is  $L$  dependent. We ignore the  $L$  dependence but use the  $S$ -wave potential for all the partial waves. Since the  $D$ - and  $G$ -wave potentials of Ali-Bodmer are more attractive than the  $S$ -wave potential, this means that the present calculation favors the  $S$  wave a little more than the other waves. In most cases the Coulomb potential between the  $\alpha$  particles is switched off. If the Coulomb potential is included, the  $2\alpha$  system has a sharp  $S$ -wave resonance. The  $3\alpha$  system has only one bound state but has

TABLE I. Energies (in MeV) and root-mean-square radii (in fm) of  $N\alpha$  systems interacting via the Ali-Bodmer potential of Eq. (10). The energy is from the  $N\alpha$  threshold. Both the ground and excited states are given for  $N=3$  and 4. The result with the Coulomb force being included is indicated by an asterisk (\*). The  $\alpha$  particle is considered to be a structureless boson.  $\hbar^2/M_\alpha = 41.467/4$  MeV fm<sup>2</sup>.

$N$	Method	$E$	rms radius	Dimension
2	numerical	-1.3696	2.246	
	SVM	-1.3696	2.246	10
3		0.080*		
	ATMS [12]	-5.18	2.43	
	SVM [5]	-5.18	2.43	60
	SVM	-5.18	2.43	60
		-5.18	2.43	120
		-0.62*	2.64*	140
		-1.38	10.05	120
4	ATMS [12]	-11.1	2.65	
	SVM [5]	-11.07	2.65	150
	SVM	-11.10	2.59	150
		-11.17	2.57	450
		-5.76	3.66	450
		-2.01	5.78	450
		-0.98	6.63	450
5	SVM [5]	-16.22	2.99	400
	SVM	-18.63	2.74	480

no bound, excited  $0^+$  state. By switching off the Coulomb potential, both the ground and excited states are obtained at energies comparable to the experimental values. These results are consistent with the microscopic  $\alpha$  cluster model calculations for  $^{12}\text{C}$  [9,10]. It should be noted that there are some restrictions in the boson model. Most serious is probably that there is no way to include the effects of the Pauli principle. It is not clear how reliable the effective  $\alpha\alpha$  potential is at short distances. Reality of boson-model results should thus be accepted with some reservations, especially for those states with compact structure.

Matrix elements of most operators in the correlated Gaussians are calculated analytically. They are found in Ref. [6]. The matrix element for a nonlocal operator will be needed in the next section, so its calculation method is given in the Appendix. Calculations have been performed with the use of the computer code available in Ref. [11].

### III. RESULTS

Table I lists the energies and root-mean-square (rms) radii of  $N=2-5$   $\alpha$  particle systems. The agreement with other calculations is very good for the g.s. of  $N=3$  and 4 cases. The energy of the g.s. of the  $5\alpha$  system is considerably lower than the previous SVM result [5]. This is due to a more thorough optimization of ten parameters of the matrix  $A_i$ . The g.s. of the  $2\alpha$  system becomes a resonance if the Coulomb potential is included. The resonance energy can be calculated to a good approximation by using square integrable

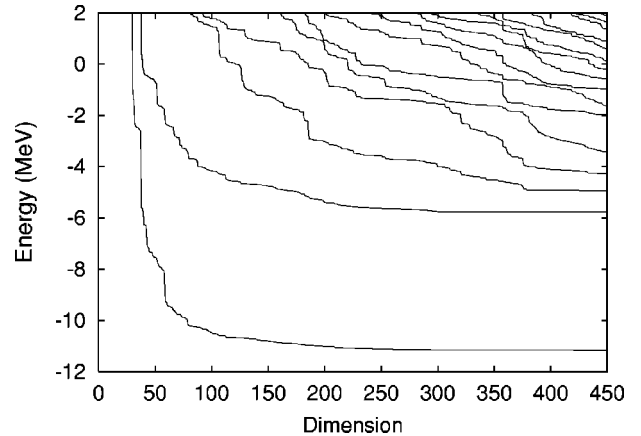


FIG. 1. Energies of  $4\alpha$  system as a function of basis dimension. The energy is measured from the  $4\alpha$  threshold.

basis if the resonance has a sharp width. For a point Coulomb potential, the resonance energy is found to be 80 keV, very close to the experimental value of 92 keV. The  $3\alpha$  system with the Coulomb potential being included becomes Borromean, that is, any pairwise constituent particles have no bound state but the three-body system has at least one (one in the present case) bound state. The g.s. energy is just 0.62 MeV below the  $3\alpha$  threshold, so one may think that this state could be identified as the excited  $0^+$  state of  $^{12}\text{C}$  at 7.65 MeV. However, this state does not have such weakly bound structure as is shown by the microscopic  $\alpha$  cluster model calculations [9,10].

When the Coulomb potential is switched off, the  $2\alpha$  system becomes bound. The energy obtained with the SVM agrees with the result of numerical solution. For the  $3\alpha$  system, two bound states are obtained: One is -5.18 MeV below the  $3\alpha$  threshold. The other is just below the  $^8\text{Be} + \alpha$  threshold. (Note that  $^8\text{Be}$  is bound.) The latter is in fact only 12 keV below the threshold, and its rms radius is as large as 10 fm. A very careful, precise calculation was needed to obtain this state. These two states may correspond to the ground and excited  $0^+$  states in  $^{12}\text{C}$ . The latter is a candidate for a  $3\alpha$  condensed state.

The energy versus basis dimension is displayed in Fig. 1 for the  $4\alpha$  system. Clearly the lowest two states well converge and they may be identified as the ground and first excited  $0^+$  states in  $^{16}\text{O}$ . The energy spacing between them is close to the experimental value, 6.16 MeV. In addition, the excited state at -5.76 MeV is located just below the  $^{12}\text{C}(\text{g.s.}) + \alpha$  threshold. The third to fifth states at  $\mathcal{K}=450$  are above the  $^{12}\text{C}(\text{g.s.}) + \alpha$  threshold and can be identified as continuum states which appear in calculations of bound-state approximation. The sixth and eighth states indicate a plateau behavior in the energy curve. We consider these states a candidate for a condensate of  $4\alpha$  particles because their energies are near the  $^{12}\text{C}(0_2^+) + \alpha$  threshold (-1.38 MeV) and the rms radii of these states are considerably large, i.e., 5.78 and 6.63 fm, respectively. Because these states are unbound and their widths are expected to be fairly large, the energies obtained by the present bound-state type calculation should not be taken very precise. A generator coordinate method (GCM)

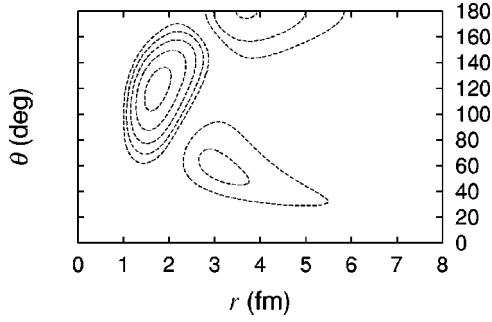


FIG. 2. Pair correlation function for the excited  $0^+$  state of  $3\alpha$  system plotted as contour maps. The positions of two  $\alpha$  particles are  $(x,y)=(r \cos \theta, r \sin \theta)$  and  $(x,y)=(r,0)$ . The position of the third  $\alpha$  particle is  $(x,y)=[-r(1+\cos \theta), -r \sin \theta]$ . The ratio of the heights between any two neighboring contour levels is three.

calculation for excited states of  $4\alpha$  system suggested the existence of a loosely coupled configuration slightly above the  $4\alpha$  threshold [13].

The excited state of  $^{12}\text{C}$  has been discussed in relation to a possible  $\alpha$ -chain state [14,15]. Several microscopic calculations based on  $3\alpha$  RGM [9] or GCM [10] reproduce both the ground and excited states reasonably well. These calculations show that the excited state does not have a particular arrangement of  $3\alpha$  particles but indicates a structure comprising various configurations as a loosely bound system. The present boson-model calculation bears it out. This conclusion has been reached by examining the pair correlation function or the two-particle density defined by

$$P(\mathbf{r}, \mathbf{r}_0) = \left\langle \Psi \left| \sum_{i \neq j} \delta(\mathbf{r}_i - \mathbf{x}_N - \mathbf{r}) \delta(\mathbf{r}_j - \mathbf{x}_N - \mathbf{r}_0) \right| \Psi \right\rangle. \quad (11)$$

Let  $\mathbf{r}_0$  be a fixed vector, pointing to a test particle positioned appropriately and let  $\mathbf{r}$  be the variable of  $P$ . The function  $P(\mathbf{r}, \mathbf{r}_0)$  shows how the fixed test particle sees the density distribution of the other particles. For a spherical state,  $P$  depends on  $|\mathbf{r}|$ ,  $|\mathbf{r}_0|$  and the angle  $\theta$  between  $\mathbf{r}$  and  $\mathbf{r}_0$ . Figure 2 shows the contour map of  $P$  for the excited state as a function of  $|\mathbf{r}|=|\mathbf{r}_0|$ , and  $\theta$ . Three peaks are clearly seen at  $\theta=60, 120$  and  $180^\circ$ . They correspond to  $2\alpha+\alpha$  ( $^8\text{Be}+\alpha$ ),  $3\alpha$  regular triangle and  $\alpha$  chain configurations, respectively. We show in Fig. 3 the pair correlation function which is obtained when the test particle is put at the distance corresponding to these peaks. When the test particle is located at  $|\mathbf{r}_0|=1.7$  fm, only a triangular configuration shows up. As  $|\mathbf{r}_0|$  increases to  $|\mathbf{r}_0|=3.1$  fm, both a linear-chain configuration and a  $^8\text{Be}+\alpha$  like configuration appear. When the test particle is located further outside ( $|\mathbf{r}_0|=3.7$  fm), a linear chain dominates.

Figure 4 compares the density distribution of the  $\alpha$  particles for the four states of  $^{16}\text{O}$ . The density distribution extends to further distances as the excitation energy increases. The reason why the central density for the g.s. is so low is because the state is compact and the Ali-Bodmer potential has a strong repulsion at short distances. This repul-

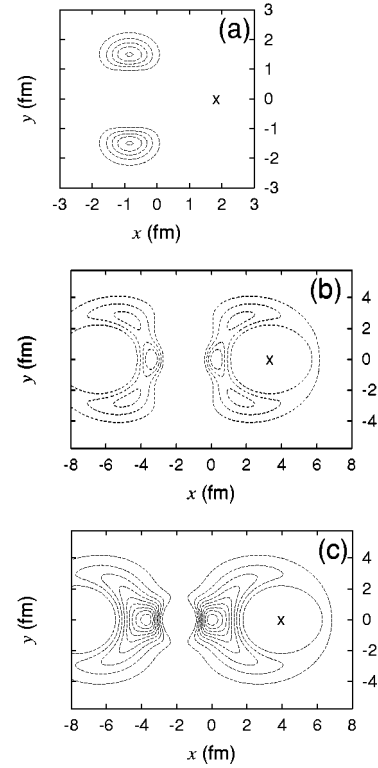


FIG. 3. Pair correlation functions for the excited  $0^+$  state of  $3\alpha$  system plotted as contour maps. The position of the test particle, marked by  $\times$ , is at  $(x,y)=(1.7 \text{ fm}, 0)$  (a),  $(x,y)=(3.1 \text{ fm}, 0)$  (b), and  $(x,y)=(3.7 \text{ fm}, 0)$  (c), respectively.

sion can be understood as a consequence of excluding Pauli-forbidden states from the effective potential [7,16].

What is a good measure to assess a condensation? A literal interpretation of an  $\alpha$  condensation is that all the  $\alpha$  particles occupy an  $S$ -wave orbit. In a finite system, the occupation probability may spread out over several orbits, but a significant probability should be occupied by a particular orbit if it is called a condensate.

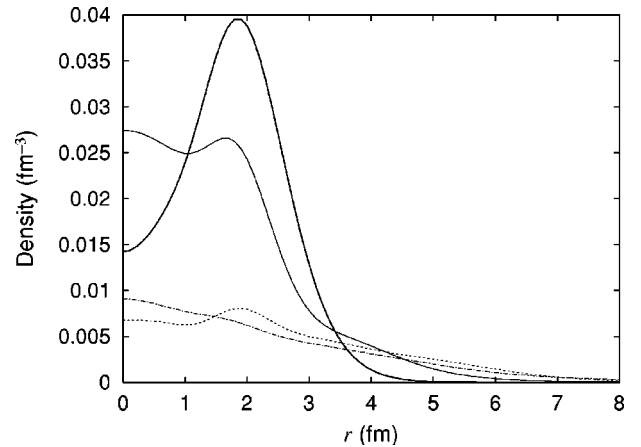


FIG. 4.  $\alpha$  particle density distributions of  $4\alpha$  system. The thick solid, thin solid, dotted, and dash-dotted curves correspond to the four states at  $-11.17, -5.76, -2.01$ , and  $-0.98$  MeV, respectively (see Table I).

The occupation probability can be calculated by solving the eigenvalue problem of a density matrix  $\rho(\mathbf{r},\mathbf{r}')$ . It is well known [17] that the density matrix for a single Slater determinant  $\Psi$  is given by

$$\rho(\mathbf{r},\mathbf{r}') \equiv N \langle \Psi | \delta(\mathbf{r}_1 - \mathbf{r}') \rangle \langle \delta(\mathbf{r}_1 - \mathbf{r}) | \Psi \rangle = \sum_c \psi_c^*(\mathbf{r}') \psi_c(\mathbf{r}), \quad (12)$$

where  $c$  runs over all the occupied orbits which constitute the Slater determinant. Since the wave function  $\Psi$  is totally antisymmetric, any single-particle coordinate  $\mathbf{r}_i$  can be used instead of  $\mathbf{r}_1$  in the above equation. The eigenvalue problem of the density matrix,

$$\int d\mathbf{r}' \rho(\mathbf{r},\mathbf{r}') f(\mathbf{r}') = \lambda f(\mathbf{r}), \quad (13)$$

gives the following solution:  $\lambda=1$  for  $f=\psi_c$  (the occupied orbit) but  $\lambda=0$  otherwise. The diagonal part of the density matrix,  $\rho(\mathbf{r},\mathbf{r})$ , is the density of the system. The sum of all the eigenvalues is equal to the number of particles  $N$  which is the trace of the density matrix,  $\int d\mathbf{r} \rho(\mathbf{r},\mathbf{r})$ .

In analogy to the above fermionic case, the density matrix for the  $N\alpha$  system may be defined as

$$\rho(\mathbf{r},\mathbf{r}') = N \langle \Psi | \delta(\mathbf{r}_1 - \mathbf{x}_N - \mathbf{r}') \rangle \langle \delta(\mathbf{r}_1 - \mathbf{x}_N - \mathbf{r}) | \Psi \rangle, \quad (14)$$

where the single  $\alpha$  particle coordinate is measured from the center-of-mass coordinate in conformity to the translation-invariant wave function  $\Psi$ . Since the wave function is totally symmetric, any single-particle coordinate  $\mathbf{r}_i$  can be used instead of  $\mathbf{r}_1$ . A spectrum of eigenvalues of the density matrix is expected to give information on the occupancy of the orbits of the system. The eigenvalues of the density matrix corresponding to an ideal condensed state would be  $N$  (just one) and zeros. A method of calculation for the density matrix is detailed in the Appendix.

The eigenvalues of the density matrices constructed from the two  $0^+$  states of  $^{12}\text{C}$  are listed in Table II. They are labeled by the sequence number  $n$  ( $=0,1,\dots$ ) and the orbital angular momentum. For the g.s., the  $0S$  eigenfunction occupies more than 80% of the total sum, and all other eigenfunctions but the  $0D$  function have small eigenvalues. For the excited state which may be a candidate of the condensed state, the eigenvalues are apparently spread out over several configurations. Though the eigenvalue of the  $0S$  orbit is largest, the occupation probability is about 40%. The sum of all the eigenvalues belonging to the  $S$ -wave eigenfunctions is about 1.6, which is approximately 50% of the total sum. The excited state of  $^{12}\text{C}$  produced by the present boson model is far from an ideal  $\alpha$  condensed state. It should be noted that the eigenfunctions of the two density matrices show quite different behavior, particularly in the spatial extension, corresponding to the different characteristics of the two states of  $^{12}\text{C}$ . This is shown in Fig. 5 where four eigenfunctions that have largest eigenvalues are displayed. Table II also lists the eigenvalues of the density matrix for the g.s.

TABLE II. Eigenvalues of the density matrix for  $3\alpha$  system. The eigenvalue  $\lambda$  is labeled by the sequence number  $n$  and the angular momentum  $L$  of the corresponding eigenfunction. The result with the Coulomb force is indicated by an asterisk (\*).

$0_1^+(-5.18)$		$0_2^+(-1.38)$		$0_1^+(-0.62)^*$	
$nL$	$\lambda$	$nL$	$\lambda$	$nL$	$\lambda$
$0S$	2.447	$0S$	1.287	$0S$	2.505
$0D$	0.363	$0D$	0.482	$0D$	0.304
$0P$	0.075	$1S$	0.287	$0P$	0.072
$1S$	0.063	$0P$	0.157	$1S$	0.066
$0F$	0.013	$0G$	0.128	$0G$	0.012
$0G$	0.012	$1D$	0.106	$0F$	0.010
$1P$	0.008	$2S$	0.049	$1P$	0.008
$1D$	0.007	$2D$	0.048	$1D$	0.007
$1G$	0.005	$0I$	0.041	$1G$	0.007
$0I$	0.001	$1G$	0.038	$2S$	0.002
$0H$	0.001	$1P$	0.026	$0I$	0.001

which is obtained by switching on the Coulomb potential. The spectrum of the eigenvalues is similar to the case for the no-Coulomb g.s.

The eigenvalues of the density matrices for the  $4\alpha$  system are presented in Table III. The general behavior of the spectrum for the two lowest states is similar to the  $3\alpha$  case. The g.s. might be called an  $\alpha$  condensed state because the eigen-

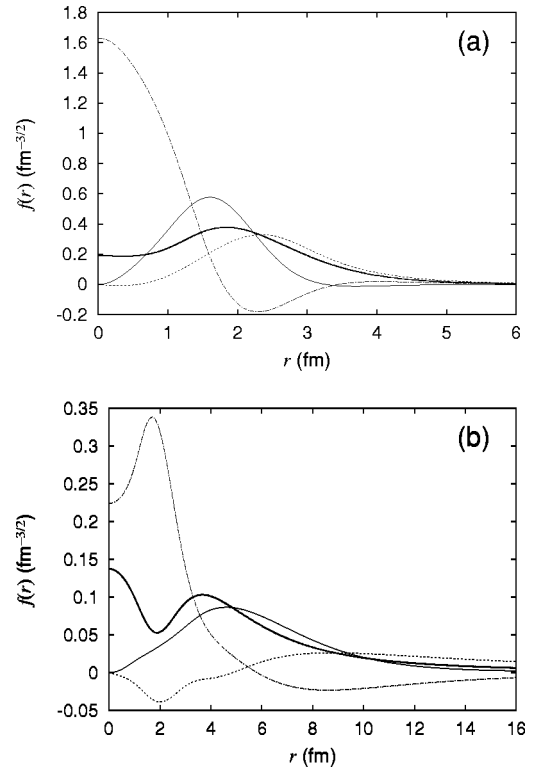


FIG. 5. Radial parts of the eigenfunctions of the density matrix of  $3\alpha$  system. (a) is for the g.s. and (b) is for the excited  $0^+$  state. The thick solid, thin solid, dotted, and dash-dotted curves denote the eigenfunctions with  $0S$ ,  $0D$ ,  $0P$ , and  $1S$ , respectively.

TABLE III. Eigenvalues of the density matrix for  $4\alpha$  system. See the caption of Table II.

$0_1^+(-11.17)$		$0_2^+(-5.76)$		$0^+(-2.01)$		$0^+(-0.98)$	
$nL$	$\lambda$	$nL$	$\lambda$	$nL$	$\lambda$	$nL$	$\lambda$
0S	2.815	0S	1.994	0S	1.180	0S	1.611
0D	0.520	1S	0.830	0P	1.114	0D	0.716
0P	0.203	0D	0.354	0D	0.432	1S	0.525
0F	0.173	0P	0.181	1S	0.277	0P	0.317
1P	0.114	1P	0.115	2S	0.140	1P	0.163
1S	0.073	1D	0.112	1D	0.134	0F	0.108
0G	0.022	0F	0.095	0F	0.109	2S	0.071
1D	0.015	0G	0.069	1P	0.087	1D	0.061
1G	0.011	2P	0.057	2P	0.045	2P	0.041
1F	0.008	2S	0.053	0G	0.040	0G	0.039
0H	0.007	0H	0.023	0H	0.038	3S	0.032
2S	0.007	1F	0.016	1F	0.034	1F	0.031

value of the 0S orbit is about 70% of the total sum, but that state is considered to correspond to the doubly magic g.s. of  $^{16}\text{O}$ . Thus this is just an artifact of the boson model. The excited state at  $-2.01$  MeV is conjectured to be a candidate of the condensation, but its  $P$ -wave eigenvalue is as large as the lowest  $S$ -wave eigenvalue. The excited state at  $-0.98$  MeV has stronger concentration in an  $S$  orbit, but the occupancy of the 0S orbit is about 40%. Thus it is likely that either of these is not an  $\alpha$  condensed state.

#### IV. SUMMARY

The possibility of  $\alpha$  condensation in  $^{12}\text{C}$  and  $^{16}\text{O}$  was investigated in an  $\alpha$ -boson model. Variational solutions for  $0^+$  states of  $3\alpha$  and  $4\alpha$  systems were obtained by the stochastic optimization of the nonlinear parameters of the correlated Gaussian basis. The precision of the calculation was good enough to discuss the  $\alpha$  condensation.

Some states with large spatial extension were found near the  $\alpha$  threshold in both  $^{12}\text{C}$  and  $^{16}\text{O}$ . To assess the measure of condensation, the occupation probabilities of various single  $\alpha$  particle orbits were calculated by diagonalizing the density matrix constructed from the state of interest. The results of analysis indicated that the candidate is far from an ideal  $\alpha$  condensed state. For example, the probability that the  $3\alpha$  system remains in a single  $S$  orbit was at most 40% in spite of the fact that the system is in an extremely extended state.

We used the  $\alpha$  boson model. It obviously has some limitations from the viewpoint of microscopic nuclear structure models. The boson model may not work well for the ground states of  $^{12}\text{C}$  and  $^{16}\text{O}$ , thereby causing some undesirable influence on the excited states. To obtain more definitive conclusion, realistic calculations must be performed at the nucleon level in which no  $\alpha$  cluster assumption is invoked. A 12-nucleon calculation which reproduces both the ground and excited  $0^+$  states of  $^{12}\text{C}$  at the correct energies will enable one to quantify the degree to which the  $\alpha$  clusters, if a condensation is the case, are condensed in the excited state.

#### ACKNOWLEDGMENT

The authors would like to thank P. Schuck for useful suggestions and discussions.

#### APPENDIX: CALCULATION OF DENSITY MATRIX

The aim of this appendix is to show a method of calculation for the density matrix (14). It is considered a matrix element of a special nonlocal operator,  $|\delta(\mathbf{r}_1 - \mathbf{x}_N - \mathbf{r}')\rangle\langle\delta(\mathbf{r}_1 - \mathbf{x}_N - \mathbf{r})|$ , where  $\mathbf{x}_N$  is the center-of-mass coordinate of the system. It should be noted that  $\mathbf{y}_1 \equiv \mathbf{r}_1 - \mathbf{x}_N$  may not belong to a member of the coordinate set  $\mathbf{x}$ , which is used to define the correlated Gaussian (4). A most direct but tedious way of the calculation of the matrix element of  $|\delta(\mathbf{y}_1 - \mathbf{r}')\rangle\langle\delta(\mathbf{y}_1 - \mathbf{r})|$  is to express  $\mathbf{y}_1$  in terms of the set  $\mathbf{x}$ , and then to perform the integration over these coordinates. Here we take another route.

The first step of the calculation is to transform the coordinates  $\mathbf{x} = \{\mathbf{x}_1, \mathbf{x}_2, \dots, \mathbf{x}_{N-1}\}$  to a new set of coordinates  $\mathbf{y} = \{\mathbf{y}_1, \mathbf{y}_2, \dots, \mathbf{y}_{N-1}\}$ :

$$\mathbf{y}_i = \sum_{k=1}^{N-1} (w^{(i)})_k \mathbf{x}_k = \widetilde{w^{(i)}} \mathbf{x}. \quad (\text{A1})$$

The symbol  $\widetilde{\phantom{x}}$  indicates the transposition of a matrix or a vector. The  $(N-1)$ -dimensional column vector  $w^{(1)}$  is chosen in such a way that the first coordinate  $\mathbf{y}_1$  reduces to the one defined above. The choice of the other coordinates  $\{\mathbf{y}_2, \dots, \mathbf{y}_{N-1}\}$  is, however, not unique and thus the column vectors  $w^{(i)}$  ( $i=2, \dots, N-1$ ) are not unique, either. For the sake of convenience, we may require that these  $(N-2)$  vectors be all normalized and orthogonal to each other and, moreover, orthogonal to  $w^{(1)}$  as well. The vectors  $w^{(i)}$  form a complete set in a real vector space of  $(N-1)$  dimension.

The coordinate transformation (A1) from  $\mathbf{x}$  to  $\mathbf{y}$  is expressed as  $\mathbf{y} = T^{-1}\mathbf{x}$  by a matrix  $T^{-1}$ , where  $\mathbf{y}$  (and also  $\mathbf{x}$ ) is considered a column vector comprising  $\{\mathbf{y}_i\}$  (and also  $\{\mathbf{x}_i\}$ ). The inverse transformation from  $\mathbf{y}$  to  $\mathbf{x}$ ,  $\mathbf{x} = T\mathbf{y}$ , is performed by the matrix  $T$ ,

$$T = (w^{(1)} w^{(2)} \dots w^{(N-1)}) \begin{pmatrix} \frac{1}{\mu_1} & 0 \\ 0 & I_{N-2} \end{pmatrix}. \quad (\text{A2})$$

Here  $\mu_1 = \widetilde{w^{(1)}} w^{(1)}$  and  $I_n$  is an  $n \times n$  unit matrix. The Jacobian for the transformation becomes  $|\det(\partial\mathbf{x}/\partial\mathbf{y})| = |\det T|^3 = \mu_1^{-3} |\det \widetilde{T^{-1}}|^3 = \mu_1^{-3} |\det(T^{-1} \widetilde{T^{-1}})|^{3/2} = \mu_1^{-3/2}$ .

The next step is to calculate the matrix element of  $|\delta(\mathbf{y}_1 - \mathbf{r}')\rangle\langle\delta(\mathbf{y}_1 - \mathbf{r})|$  between the correlated Gaussians (4). In what follows we extend this correlated Gaussian to a more general one:

$$\begin{aligned} g(s; A, \mathbf{x}) &= \exp\left(-\frac{1}{2} \sum_{ij} A_{ij} \mathbf{x}_i \cdot \mathbf{x}_j + \sum_i s_i \cdot \mathbf{x}_i\right) \\ &= \exp\left(-\frac{1}{2} \widetilde{\mathbf{x}} A \mathbf{x} + \widetilde{\mathbf{s}} \mathbf{x}\right), \end{aligned} \quad (\text{A3})$$

where  $\mathbf{s} = \{s_1, s_2, \dots, s_{N-1}\}$  is a set of vectors which serves to generate a correlated Gaussian with nonspherical shape [5,6]. The correlated Gaussian  $G$  is simply obtained by putting  $s=0$  in  $g$ . By substituting  $\mathbf{x} = T\mathbf{y}$  in Eq. (A3), the function  $g$  is transformed to

$$g(\mathbf{s}; A, \mathbf{x}) = g(\tilde{T}\mathbf{s}; \tilde{T}AT, \mathbf{y}), \quad (\text{A4})$$

which leads to

$$\langle \delta(\mathbf{y}_1 - \mathbf{r}) | g(\mathbf{s}; A, \mathbf{x}) \rangle = \exp\left(-\frac{1}{2}a_1\mathbf{r}^2 + \mathbf{t}_1 \cdot \mathbf{r}\right) \times g(\mathbf{t}^{(1)} - a^{(1)}\mathbf{r}; A^{(1)}, \mathbf{y}^{(1)}), \quad (\text{A5})$$

with the use of short-hand notations for the matrix  $\tilde{T}AT$ , the vectors  $(\tilde{T}\mathbf{s})_i$  ( $i=1, \dots, N-1$ ), and  $\mathbf{y}^{(1)}$ ,

$$\tilde{T}AT = \begin{pmatrix} a_1 & \tilde{a}^{(1)} \\ a^{(1)} & A^{(1)} \end{pmatrix}, \quad \tilde{T}\mathbf{s} = \begin{pmatrix} \mathbf{t}_1 \\ \mathbf{t}^{(1)} \end{pmatrix}, \quad \mathbf{y}^{(1)} = \begin{pmatrix} \mathbf{y}_2 \\ \vdots \\ \mathbf{y}_{N-1} \end{pmatrix}. \quad (\text{A6})$$

Here  $a_1$  and  $\mathbf{t}_1$ , for example, are given by

$$a_1 = \frac{1}{\mu_1} \widetilde{w^{(1)}Aw^{(1)}}, \quad \mathbf{t}_1 = \frac{1}{\mu_1} \widetilde{w^{(1)}s}. \quad (\text{A7})$$

Note that  $a^{(1)}$  is an  $(N-2)$ -dimensional column vector,  $A^{(1)}$  an  $(N-2) \times (N-2)$  symmetric matrix, and  $\mathbf{t}^{(1)}$  is an  $(N-2)$ -dimensional column vector whose  $i$ th element is  $(\tilde{T}\mathbf{s})_{i+1}$ .

Using Eq. (A5) and integrating over  $\mathbf{y}_2, \dots, \mathbf{y}_{N-1}$  leads to the following result:

$$\begin{aligned} & \langle g(\mathbf{s}'; A', \mathbf{x}) | \delta(\mathbf{y}_1 - \mathbf{r}') \rangle \langle \delta(\mathbf{y}_1 - \mathbf{r}) | g(\mathbf{s}; A, \mathbf{x}) \rangle \\ &= \left( \frac{(2\pi)^{N-2}}{\mu_1 \det B^{(1)}} \right)^{3/2} \exp\left(-\frac{1}{2}a_1\mathbf{r}^2 + \mathbf{t}_1 \cdot \mathbf{r}\right) \\ & \quad - \frac{1}{2}a'_1\mathbf{r}'^2 + \mathbf{t}'_1 \cdot \mathbf{r}' + \frac{1}{2}\tilde{\mathbf{v}}(B^{(1)})^{-1}\mathbf{v} \end{aligned} \quad (\text{A8})$$

with

$$\begin{aligned} B^{(1)} &= A^{(1)} + A'^{(1)}, \\ \mathbf{v} &= \mathbf{t}^{(1)} - a^{(1)}\mathbf{r} + \mathbf{t}'^{(1)} - a'^{(1)}\mathbf{r}', \end{aligned} \quad (\text{A9})$$

where the primed quantities such as  $a'_1$ ,  $a'^{(1)}$ ,  $\mathbf{t}'_1$ ,  $\mathbf{t}'^{(1)}$  are defined through  $A'$  and  $\mathbf{s}'$  in exactly the same way as in Eqs. (A6) and (A7). Equation (A8) is the desired formula to calculate the density matrix. By setting  $\mathbf{s}'=0$  and  $\mathbf{s}=0$  in Eq. (A8), we obtain the required matrix element for the correlated Gaussians  $G$ .

The formula (A8) may seem to depend on the choice of the vectors  $w^{(i)}$  ( $i=2, \dots, N-1$ ) because, e.g., the matrix  $B^{(1)}$  apparently depends on them. The dependence on  $w^{(i)}$  cannot be accepted because the quantity we are calculating should entirely be defined by  $w^{(1)}$  alone. The relevant quantities in Eq. (A8) are in fact independent of the choice of  $w^{(i)}$  but determined by  $w^{(1)}$  alone as follows:

$$\begin{aligned} \det B^{(1)} &= \frac{1}{\mu_1} \widetilde{w^{(1)}B^{-1}w^{(1)}} \det B, \\ \tilde{\mathbf{v}}(B^{(1)})^{-1}\mathbf{v} &= \tilde{\mathbf{z}}C\mathbf{z}, \end{aligned} \quad (\text{A10})$$

with

$$\begin{aligned} B &= A + A', \quad C = B^{-1} \\ & \quad - \frac{1}{\widetilde{w^{(1)}B^{-1}w^{(1)}}} B^{-1}w^{(1)}\widetilde{w^{(1)}B^{-1}}, \\ \mathbf{z} &= \mathbf{s} + \mathbf{s}' - \frac{1}{\mu_1}Aw^{(1)}\mathbf{r} - \frac{1}{\mu_1}A'w^{(1)}\mathbf{r}'. \end{aligned} \quad (\text{A11})$$

The proof is available from the authors at the email address [suzuki@nt.sc.niigata-u.ac.jp](mailto:suzuki@nt.sc.niigata-u.ac.jp). We note that the method of calculation for the density matrix can readily be applicable to the calculation of matrix elements of a nonlocal operator  $|\delta(\mathbf{r}_k - \mathbf{r}_l - \mathbf{r}')\rangle \langle \delta(\mathbf{r}_k - \mathbf{r}_l - \mathbf{r})|$  by simply changing  $\mathbf{y}_1$  as  $\mathbf{y}_1 = \mathbf{r}_k - \mathbf{r}_l$ .

[1] K. Wildermuth and Y. C. Tang, *A Unified Theory of the Nucleus* (Vieweg, Braunschweig, 1977).  
 [2] K. Ikeda *et al.*, *Comprehensive Study of Structure of Light Nuclei* [Suppl. Prog. Theor. Phys. **68** (1980)].  
 [3] A. Tohsaki, H. Horiuchi, P. Schuck, and G. Röpke, Phys. Rev. Lett. **87**, 192501 (2001).  
 [4] P. Navrátil, J. P. Vary, and B. R. Barrett, Phys. Rev. Lett. **84**, 5728 (2000).  
 [5] K. Varga and Y. Suzuki, Phys. Rev. C **52**, 2885 (1995).  
 [6] Y. Suzuki and K. Varga, *Stochastic Variational Approach to*

*Quantum-Mechanical Few-Body Problems* (Springer, Berlin, 1998).  
 [7] S. Saito, Prog. Theor. Phys. **40**, 893 (1968); **41**, 705 (1969).  
 [8] S. Ali and A. R. Bodmer, Nucl. Phys. **80**, 99 (1966).  
 [9] Y. Fukushima and M. Kamimura, J. Phys. Soc. Jpn. **44**, 225 (1978); M. Kamimura, Nucl. Phys. **A351**, 456 (1981).  
 [10] E. Uegaki, Y. Abe, S. Okabe, and H. Tanaka, Prog. Theor. Phys. **59**, 1031 (1978); **62**, 1621 (1979).  
 [11] K. Varga and Y. Suzuki, Comput. Phys. Commun. **106**, 157 (1997).

- [12] Y. Akaishi, *International Review of Nuclear Physics* (World Scientific, Singapore, 1986), Vol. 4, p. 259.
- [13] Y. Suzuki, *Prog. Theor. Phys.* **64**, 2041 (1980).
- [14] H. Morinaga, *Phys. Rev.* **101**, 254 (1956); *Phys. Lett.* **21**, 78 (1966).
- [15] K. Ikeda, N. Takigawa, and H. Horiuchi, *Suppl. Prog. Theor. Phys.* **Extra Number**, 464 (1968).
- [16] D. Baye, *Phys. Rev. Lett.* **58**, 2738 (1987).
- [17] P. Ring and P. Schuck, *The Nuclear Many-Body Problem* (Springer, Berlin, 1980).